# Optimization Studies of the CERN-ISOLDE neutron converter and fission target system

**Raul Luís[1], José G. Marques, Thierry Stora, Pedro Vaz, Luca Zanini**
[1]ITN – Estrada Nacional 10, 2686-953, Sacavém, Portugal
[2]CERN – CH-1211, Genève 23, Switzerland
[3]PSI – 5232 Villigen, Switzerland

E-mail: raulfluis@itn.pt

**Abstract.** The ISOLDE facility at CERN has been one of the leading isotope separator on-line (ISOL) facilities worldwide since it became operative in 1967. More than 1000 isotopes are available at ISOLDE, produced after the bombardment of various primary targets with a pulsed proton beam of energy 1.4 GeV and an average intensity of 2 μA. A tungsten solid neutron converter has been used for ten years to produce neutron-rich fission fragments in $UC_x$ targets. In this work, the Monte Carlo code FLUKA and the cross section codes TALYS and ABRABLA were used to study the current layout of the neutron converter and fission target system of the ISOLDE facility. An optimized target system layout is proposed, which maximizes the production of neutron-rich isotopes and reduces the contamination by undesired proton-rich isobars. The studies here reported can already be applied to ISOLDE and will be of special relevance for the future facilities HIE-ISOLDE and EURISOL.

## 1. Introduction

One of the most efficient ways to study nuclei far from stability is the Isotope Separation On-Line (ISOL) method, in which a beam of high-energy hadrons hits a thick target, producing a great variety of radioactive products through different processes like fission, spallation and fragmentation [1]. The resulting nuclides can be studied after they are extracted from the target, ionized and mass separated.

The ISOLDE facility at CERN has been one of the leading facilities worldwide for the production of radioactive ion beams (RIBs) using the ISOL method, since it started operating in 1967 [2,3]. Operational since 2001, the facility for accelerated RIBs at ISOLDE, REX-ISOLDE (REX-Radioactive beam EXperiment) [3], consists of a normal conducting linear accelerator with the potential to accelerate up to 3.5 MeV/u most of the 1000 radioactive isotopes produced by the bombardment of various primary targets with a 1.4 GeV proton beam (2 μA, on average) from the PS Booster [4].

The HIE-ISOLDE project [5] foresees a major upgrade of the ISOLDE facility, aiming at expanding the physics program of REX-ISOLDE with higher beam energies and intensities, with improved quality and flexibility. The existing REX accelerating structure will be replaced by a superconducting (SC) linear accelerator that can deliver a maximum energy of 10 MeV/u for a mass-to-charge ratio A/Q=4.5, an improvement that will open a broad programme of nuclear structure and nuclear astrophysics studies using different classes of nuclear reactions. HIE-ISOLDE will represent,

[1] To whom any correspondence should be addressed.

along with SPES at INFN-LNL (Italy) and SPIRAL2 at GANIL (France), a step forward towards the ultimate European ISOL facility, EURISOL [6].

The current configuration of the ISOLDE neutron converter and fission target system, which has been used for ten years at ISOLDE to produce neutron-rich fission fragments, was studied in detail in this work, using the state-of-the-art Monte Carlo code FLUKA [7] and the cross section codes TALYS [8] and ABRABLA [9, 10]. An optimization of the existing system is here proposed, to maximize the production of important neutron-rich isotopes while reducing undesired backgrounds of proton-rich isobars. The proposed optimization can already be applied to ISOLDE and will be of special relevance for HIE-ISOLDE, since the planned increase in proton beam energy (from 1.4 to 2 GeV) will result in larger fractions of produced backgrounds.

## 2. Objectives and methods

The main regions of interest for this work in the nuclear landscape lie in or near the double shell closures of $^{78}$Ni and $^{132}$Sn. Knowledge of the properties of nuclides beyond the nuclear shell closures in exotic nuclei is very important for a fundamental understanding of nuclear structure or to determine the path of the r-process, responsible for the nucleosynthesis of about half of the heavy elements [14,15]. In these regions, Zn, Ga, Cu, and Cd isotopes are preferred since they have the most appropriate release properties for the target materials currently used at ISOLDE. In this study, focus is given to zinc and cadmium isotopes, namely $^{80}$Zn and $^{130}$Cd, which lie in the neutron shell closures N=50 and N=82, respectively.

The first objective of this work was to calculate in-target yields of neutron-rich isotopes of zinc and cadmium using FLUKA, after a detailed implementation of the geometry and constituent materials of the production layout, including the target-ion source system and surrounding structures. This was done for two different configurations currently used at ISOLDE, shown in Figure 1 (as implemented in FLUKA):

- In the first configuration (left), the 1.4 GeV proton beam hits a UCx target, producing, by fission, spallation and fragmentation reactions, a large variety of radioactive products, to be ionized, mass-separated and accelerated at a later stage;
- In the second configuration (right), the proton beam hits a solid tungsten converter, generating intense neutron fluences through spallation processes. These neutrons induce fission in the UCx target, placed close to the spallation target, generating the desired radioactive products.

When the direct beam configuration is used, fission is induced mainly by GeV protons and there is a strong contribution of spallation-fission, meaning that many of the target nuclei will first evaporate a significant number of neutrons and protons and then fission at a later stage. This leads to a shift of the fission yields towards neutron-deficient species, which means that there will be a background of proton-rich isobars when the aim is to produce neutron-rich species. To avoid this background, low-energy fission can be used [16,17]. At ISOLDE, a solid tungsten “neutron converter” has been used for several years to obtain MeV neutrons from the incident proton beam, which induce fission in the UCx target (converter configuration). However, reduced beam intensities result from the present layout of the converter configuration, in comparison with the yields obtained with the direct beam configuration [18].

The uranium carbide target is 20 cm long and has a radius of 0.7 cm (approximate volume of 31 cm$^3$), while the tungsten converter is 12.5 cm long and has a 0.6 cm radius. The $UC_x$ target is composed of several pellets, each made of depleted uranium carbide phases dispersed in a matrix of graphite, packed tightly inside a tantalum container. For the simulations the fissile material was described as approximately homogeneous, with a density of 3.5 g/cm$^3$ (average density of the real target). A radial Gaussian distribution with $\sigma$=3.5 mm was assumed for the proton beam, to match the experimental conditions.

After validation of the computational yields against experimental data, an optimization of the target system layout was carried out to increase the production of the neutron-rich isotopes $^{80}$Zn and $^{130}$Cd while reducing the contamination by the respective proton-rich isobars $^{80}$Rb and $^{130}$Cs.

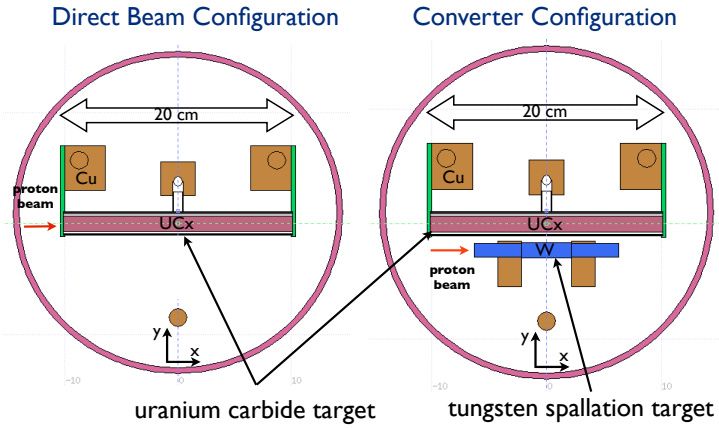


**Figure 1 –** Direct beam configuration (left) and converter configuration (right) of the ISOLDE target system

## 3. Results and discussion

*3.1. Comparison between experimental and computational yields*

Figure 2 shows the comparison between the experimental yields (from the ISOLDE database) and the computational yields, for Zinc isotopes in both direct (left) and converter (right) configurations. There is also a comparison between the yields obtained with FLUKA cross sections and the yields obtained with the TALYS + ABRABLA combination. For the latter case, FLUKA was used to obtain the proton and neutron track-length fluence spectra in the $UC_x$ target (average fluences over the target volume), and these fluences were later multiplied by the calculated cross-sections and number of target atoms, to obtain the in-target yields. In both cases, the yields are multiplied by the release efficiencies and an assumed ionization efficiency of 10% (no accurate experimental value was available).

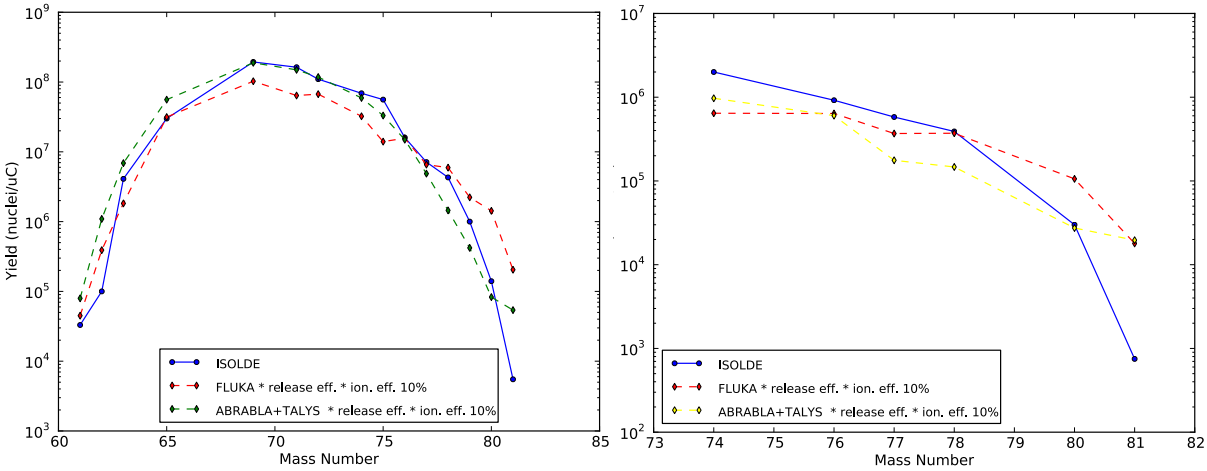


**Figure 2** - Comparison between Zinc isotope yields obtained with FLUKA and ABRABLA + TALYS cross sections, for the direct (left) and converter (right) configurations.

For most isotopes, the yields obtained with TALYS + ABRABLA cross sections are closer to the experimental yields than the ones obtained with FLUKA. In spite of this better agreement, there are still sizable discrepancies for $^{62}$Zn and $^{81}$Zn. These discrepancies might be related to the release properties of these isotopes or to uncertainties in the production cross sections. Since a better agreement was achieved with the ABRABLA + TALYS cross-sections, these were chosen over the

FLUKA cross sections for the rest of this work. Nevertheless, all calculations were also done using FLUKA cross sections, and these results will be mentioned when appropriate.

To further determine an ionization efficiency that better matches the experimental and computational results, the sum of the squared relative differences between the experimental and calculated yields was minimized, with the ionization efficiency as the free parameter [19]. For this calculation, the results for $^{81}$Zn and $^{62}$Zn were excluded, since they have very large deviations from the experimental values, as can be seen in Figure 2. An ionization efficiency of 8.1 % was thus determined, close to the efficiency values obtained in typical "offline" efficiency measurements. Using this efficiency value there is, in the direct configuration, a maximum in the ratio experimental/computational results of 3.7, for $^{78}$Zn. For $^{79}$Zn this ratio has a value of 2.9, and for the remaining isotopes the experimental and computational differ by less than a factor of 2. In the converter configuration the ratio experimental/computational reaches 4.1 for $^{77}$Zn, 3.3 for $^{78}$Zn and 2.5 for $^{74}$Zn (below 2 for the remaining isotopes). Even though there are still significant deviations between the experimental and computational results for some isotopes, this can be considered a good benchmark, if the difficulties imposed by the uncertainties in the efficiencies, cross sections and experimental yields are taken into account.

### *3.2. Optimization Studies*

*3.2.1. Particle fluences in the $UC_x$ target – standard converter configuration.* As previously stated, the main objective of the optimization studies described in this section was to propose a new geometry for the converter configuration of the ISOLDE target system, that maximized the yields of the neutron-rich isotopes $^{80}$Zn and $^{130}$Cd (and beyond, towards more neutron-rich nuclides, if possible) while reducing as much as possible the yields of the proton-rich contaminants $^{80}$Rb and $^{130}$Cs. The first step consisted in calculating the yields of several isotopes of zinc, rubidium, cadmium and cesium for the standard converter configuration. Simulation results show 4.69E5 nuclei of $^{80}$Zn formed in the $UC_x$ target for each μC of protons hitting the converter, while the yield of $^{80}$Rb is approximately the double of that value (9.5E5 nuclei/μC). For $^{130}$Cd, there are 1.3E6 nuclei/μC formed in the target, against 1.1E7 nuclei/μC of $^{130}$Cs, the proton-rich contaminant. This means that the yield of the contaminant is in both cases higher than the yield of the desired nuclide. For isotopes like $^{81}$Zn and $^{82}$Zn or $^{131}$Cd and $^{132}$Cd the contamination by proton-rich isobars is even greater. It is the objective of this work to reduce as much as possible the yields of the mentioned contaminants while maximizing the production of the desired species.

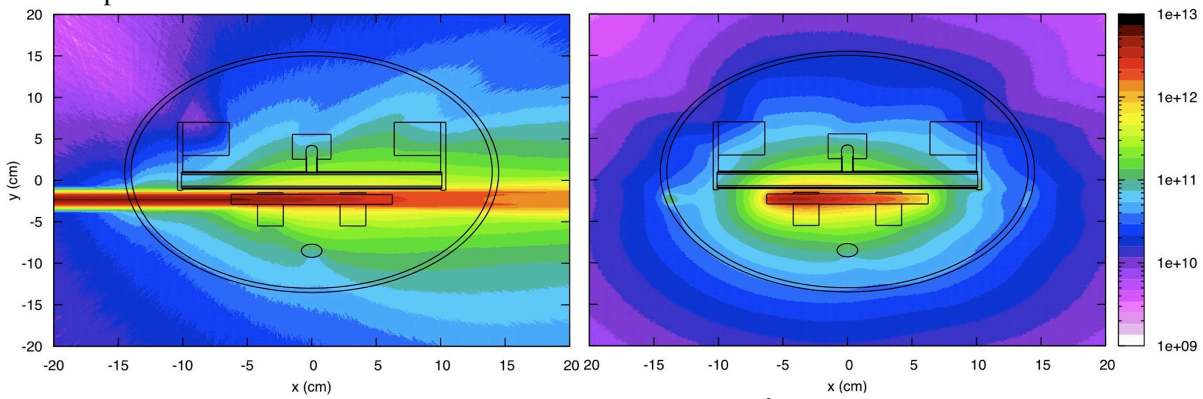


**Figure 3** – Proton (left) and neutron (right) fluence maps (1/cm$^2$/μC) obtained with FLUKA, for the converter configuration.

In Section 2 it was mentioned that the converter is used so that fission is induced by neutrons in the MeV region and not by GeV protons, thus reducing the number of proton-rich nuclei (contaminants) formed through spallation-fission. Figure 11 shows the proton (left) and neutron (right) fluence maps

computed with FLUKA in the targets zone of the converter configuration. It is clearly seen that the proton fluences in the $UC_x$ target are still considerable, especially in the rightmost part of the target. These are very energetic protons that were scattered in the converter, spreading with an approximate "conical shape" in the direction of incidence of the proton beam. The spallation neutrons spread with an approximate isotropic distribution around the converter. The optimization of the target system was based on the different spatial distributions of the neutron and proton fluences.

*3.2.2. First optimized geometry*. Figure 4 shows the first optimized target configuration. The length of the $UC_x$ target was reduced from 20 cm to 10 cm, to remove the region with the highest proton fluences, and an additional diagonal cut was made to the target, for the same reason. To compensate for the loss in volume, the target radius was increased from 0.7 cm to 1.5 cm. The tungsten converter radius was also increased. Tungsten is almost transparent to neutrons and, as it is a heavy material (Z=74), it is efficient to stop protons. A thicker converter will have several advantages, since it will stop more protons while being a brighter neutron source. Several converter thicknesses were tested, and a 1.4 cm thickness was chosen, up from 0.6 cm in the current ISOLDE configuration.

The effect of this optimization can be seen in Figure 4, which shows the neutron and proton differential fluences as a function of energy entering the $UC_x$ target. Clearly, there is a drastic reduction in the proton fluences, especially for energies in the GeV region, while the neutron fluences at lower energies are less affected. Having increased the number of $^{238}U$ atoms exposed to these neutrons, it could be anticipated that the yields of the neutron-rich isotopes would be much less affected than the yields of proton-rich contaminants.

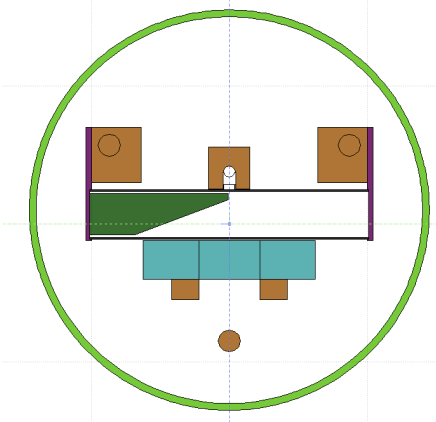

**Figure 4.** First optimized geometry

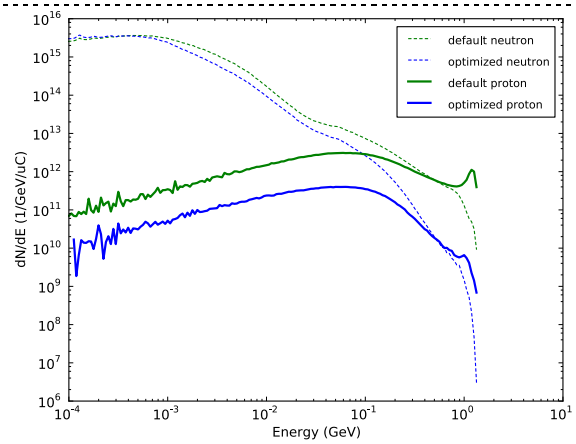


**Figure 5.** – Neutron and proton fluences (1/GeV/μC) in the $UC_x$ target for the optimized geometry

Figure 6 shows the yields of zinc and rubidium isotopes in the $UC_x$ target before and after optimization. The ratios between optimized and default yields are presented in Figure 7, along with the improvement in the zinc/rubidium ratio. The yield of $^{80}Zn$, one of the reference nuclides for this work, is reduced to 54% of its original value, while the yield of the contaminant $^{80}Rb$ is decreased to 1.4% of its value in the current configuration. Overall, the $^{80}Zn/^{80}Rb$ ratio is increased by a factor 39, a result that gives good indications that it is possible to produce purer and more intense beams of neutron-rich zinc isotopes with simple changes in the targets layout. This ratio will of course be maintained in the final radioactive ion beam. These calculations were repeated using FLUKA cross sections and the predicted improvements were similar.

The same calculations were performed for Cadmium and Cesium isotopes. The yield of $^{130}Cd$ is reduced by 40% while the yield of $^{130}Cs$ is reduced to 3.3 % of its original value. The ratio $^{130}Cd/^{130}Cs$ ratio is increased 18 times after optimization, which also represents an important improvement.

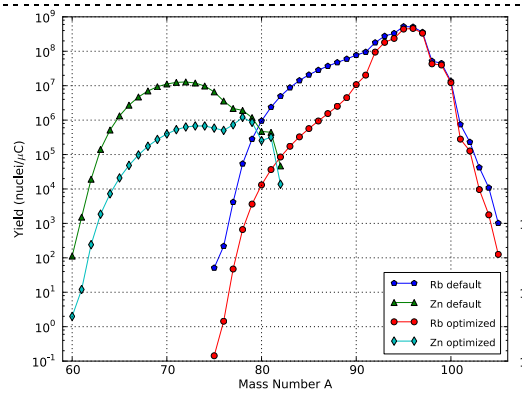


**Figure 6.** Zinc and rubidium yields (nuclei/ μC) before and after optimization.

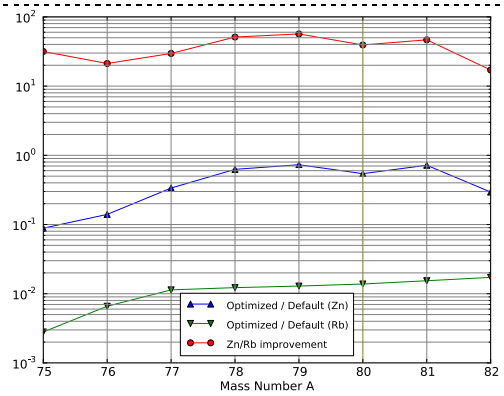


**Figure 7.** Improvement in the zinc/rubidium ratios.

Although the proposed optimization looks promising, there is a possible drawback, related to the release efficiency of the produced isotopes from the target. The $UC_x$ target radius was increased to compensate for the reduction in target length, and the result was an increased target volume in the proposed configuration. Therefore, the release efficiency will probably be reduced, affecting the intensity of the final RIB. To address this possible issue, an alternative configuration for the target system was tested.

*3.2.3. Further optimizations – $UC_x$ target concentric to W converter*. Figure 8 shows another possible configuration for the ISOLDE targets, based on the previous optimization. The $UC_x$ target in this configuration is thinner, to enhance the release efficiency, but now it encloses the W converter completely (like a solid of revolution made with a section cut from the previous target). With this design, it is possible to increase the mass of $^{238}U$ with a thinner target, taking advantage of intercepting more neutrons than in the previous configuration. To keep the design realistic, the assumed $UC_x$ density was decreased, from an initial value of 3.5 g/cm$^3$ to 2 g/cm$^3$, since with such an exotic target it will be difficult in practice to accommodate the $UC_x$ pellets as tightly as in the current configuration. In this way, the uranium mass is approximately 2.3 times higher than in the original configuration (for a target with approximately 4 times the volume of the initial target). The same parameters of the previous optimization were considered for the W converter.

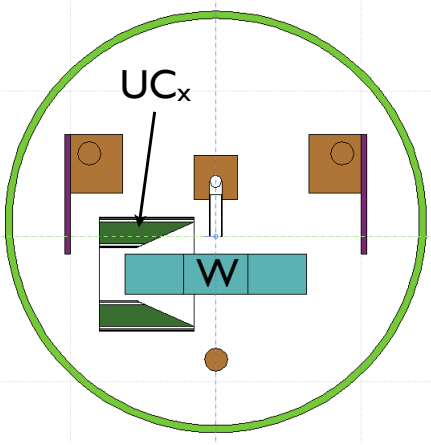


**Figure 8.** Concentric targets configuration

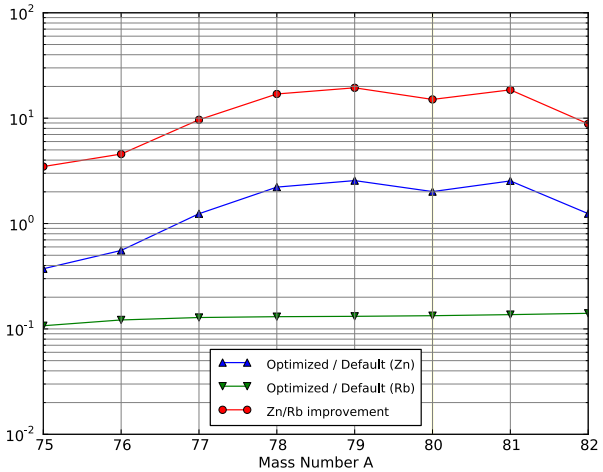


**Figure 9.** Improvement in the zinc/rubidium ratios for the concentric targets configuration

The production of $^{80}$Zn is increased by a factor 2 while the production of $^{80}$Rb is reduced to 13% of the production obtained with the default configuration (Figure 9). The result is an improvement in the $^{80}$Zn/$^{80}$Rb ratio by a factor of 15. The ratio $^{130}$Cd/$^{130}$Cs is improved by a factor 12, with the production of $^{130}$Cd being increased by a factor of 2. The main advantage of this configuration is that it will probably exhibit a higher release efficiency than the previous one. It is also important to notice that with this optimization the yields on Zn and Cd are increased when compared with the current ISOLDE targets configuration, contrasting with what is predicted with the previous optimization. Furthermore, if the density can be increased (a conservative value was used, as mentioned before), the yields of Zn and Cd will be further increased in absolute value, although the relative amount of contaminants will be the same.

## 4. Conclusions

In this work, the current configuration of the ISOLDE neutron converter and fission target system was studied in detail using the Monte Carlo code FLUKA and the cross section codes ABRABLA and TALYS, with the objective to understand the neutronics properties of the system and optimize it for the production of neutron-rich nuclides. Using the experimental yields of the ISOLDE database, a methodology was developed to perform an optimization of the targets layout in order to enhance the production of the neutron-rich isotopes $^{80}$Zn and $^{130}$Cd while reducing the production of their contaminating isobars, $^{80}$Rb and $^{130}$Cs.

The results reported in this study indicate that the ratios of $^{80}$Zn/$^{80}$Rb and $^{130}$Cd/$^{130}$Cs can be increased by more than one order of magnitude with respect to the present layout, by increasing the production of $^{80}$Zn and $^{130}$Cd and reducing the production of $^{80}$Rb and $^{130}$Cs. Additional results here reported indicate that these gains will be preserved or increased as ISOLDE moves towards higher proton beam energies, as foreseen in the HIE-ISOLDE upgrade. Since the absolute figure of merit for any radioactive ion beam facility comes from both its delivered beam intensities and their purities, this work provides a good example of how future increases of the primary beam intensities and energies at HIE-ISOLDE and EURISOL can be best exploited to deliver high rates of pure beams around the doubly magic nuclei $^{78}$Ni and $^{132}$Sn.

## References


1. Y. Blumenfeld, AIP Conf. Proc. 1024 (2010) 467-474
2. S. Galés, Nucl. Phys. A722 (2003) 148c-156c
3. O. Kester et al., Nucl. Instr. and Meth. B 204 (2003) 20–30
4. V.N. Fedosseev et al., Nucl. Instr. and Meth. B 266 (2008) 4378-4382
5. M. Lindroos et al., Nucl. Instr. and Meth. B, 266 (2008) 4687-4691
6. Y. Blumenfeld et al., Nucl. Phys. News 19(1) (2009) 22-27
7. G. Battistoni, et al., AIP Conf. Proc. 896 (2007) 31-49
8. A.J. Koning, S. Hilaire and M. Duijvestijn, TALYS-1.2 USER MANUAL, December 22, 2009
9. J. J. Gaimard and K. H. Schmidt., Nucl. Phys. A 531 (1991) 709-745
10. A.R. Junghans, Nucl. Phys. A 629 (1998) 635-655
11. http://www.phy.anl.gov/div/W_PaperF.pdf
12. Hendrik Schatz, Phys. Today 61, (2008) 40-45
13. U. Koster et al., AIP Conf. Proc. 798 (2005) 315-326
14. P Van Duppen, K. Riisager, J. Phys. G: Nucl. Part. Phys. 38 (2011)
15. R. Catherall et al., Nucl Instr Meth. B, 204 (2003), 235-239
16. T E. Cocolios, Nucl Instr Meth. B, 266 (2008), 4403-4406